

Effect of FACTS Type to Optimization Performance and Voltage Stability for Electrical Network

Marouani Ismail*, Allagui Brahim**, Hadj Abdallah Hsan***

*(Electrical department, College Of Technology, Jeddah. KINGDOM OF SAUDI ARABIA)

** (Electrical department, ENIS, 3038 Sfax, Tunisia)

*** (Electrical department, ENIS, 3038 Sfax, Tunisia)

ABSTRACT

In this paper, a multi objective evolutionary algorithm (MOEA) to solve optimal reactive power (VAR) dispatch problem with flexible AC transmission system (FACTS) devices is presented. This nonlinear multi objective problem (MOP) consists to minimize simultaneously real power loss in transmission lines and voltage deviation at load buses, by tuning parameters and location of FACTS. The constraints of this MOP are divided to equality constraints represented by load flow equations and inequality constraints such as, generation VAR sources and security limits at load buses. Two types of FACTS devices, thyristor controlled series capacitor (TCSC) and unified power flow controller (UPFC) are considered. The design problem is tested on the IEEE 30-bus system.

Keywords – Multi objective optimization; Voltage deviation; power losses; voltage stability; NSGAI; TCSC and UPFC.

I. INTRODUCTION

The VAR dispatch problem is considered as a MOP. It consists to determine the optimal voltage and minimize the real power loss in transmission lines under several equality and inequality constraints. Such as, load flow equations and security limits. To maintain the load buses voltage within their permissible limits many technical methods are proposed [1, 2]. Such as, reallocating reactive power generation in the system adjusting transformer taps, generator voltage and switchable VAR sources. But, to minimize systems losses, a redistribution of reactive power in the network can be used [2]. Because their capability to change the network parameters with a rapid response and enhanced flexibility, FACTS devices have taken more attention in power systems operations as voltage profile and minimizing system losses.

So, in first step, the objective of the present paper is to develop a power flow model for power system with FACTS devices. Then, a new VAR dispatch problem is formulated. The solutions of this problem are the FACTS parameters and location.

In the literature, several methods are used to solve a MOP. In [3, 4], a nonlinear programming technique is used. Other uses gradient-based optimization algorithms by linearizing the objective function and the system constraints around an operating point [5].

These conventional techniques consume an important computing time and they are an iterative methods. Also, they can be converged to a local optimum. So, in this paper a no conventional technique based on MOEA is used. Unlike traditional techniques,

MOEA works on a coding of the parameters to be optimized, rather than the parameters themselves. Also, it employs search procedures based on the mechanism of natural selection and survival of the fittest. So, it can converge to the global optimum solution. In our work, we opted to the use of the elitist approach NSGAI (non dominated sorting genetic algorithm) to solve the MOP.

II. FACTS DEVICES MODELS

A. Transmission line

The figure.1 shows a simple transmission line represented by its lumped Π equivalent parameters connected between bus-i and bus-j. The real and reactive power flow from bus-i to bus-j can be written as:

$$P_{ij} = V_i^2 G_{ij} - V_i V_j [G_{ij} \cos(\delta_{ij}) + B_{ij} \sin(\delta_{ij})] \quad (1)$$

$$Q_{ij} = -V_i^2 (B_{ij} + B_{sh}) - V_i V_j [G_{ij} \sin(\delta_{ij}) - B_{ij} \cos(\delta_{ij})]$$

(2)

Where $\delta_{ij} = \delta_i - \delta_j$. Similarly, the real and reactive power flow from bus-j to bus-i

$$P_{ji} = V_j^2 G_{ij} - V_i V_j [\cos(\delta_{ij}) - B_{ij} \sin(\delta_{ij})] \quad (3)$$

$$Q_{ji} = -V_j^2 (B_{ij} + B_{sh}) + V_i V_j [G_{ij} \sin(\delta_{ij}) + B_{ij} \cos(\delta_{ij})] \quad (4)$$

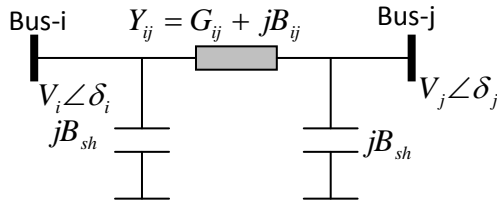


Figure 1. Transmission line mode

B. TCSC Model

Figure.2 shows the model of transmission line with TCSC connected between buses *i* and *j*. The TCSC can be considered as a static reactance $-jx_c$. The real and reactive power flow from bus-*i* to bus-*j*, and from bus-*j* to bus-*i* of a line having series impedance and a series reactance are [6]:

$$P_{ij}^{TCSC} = V_i^2 G'_{ij} - V_i V_j [G'_{ij} \cos(\delta_{ij}) + B'_{ij} \sin(\delta_{ij})] \quad (5)$$

$$Q_{ij}^{TCSC} = -V_i^2 (B'_{ij} + B_{sh}) - V_i V_j [G'_{ij} \sin(\delta_{ij}) - B'_{ij} \cos(\delta_{ij})] \quad (6)$$

$$P_{ji}^{TCSC} = V_j^2 G'_{ij} - V_i V_j [G'_{ij} \cos(\delta_{ij}) - B'_{ij} \sin(\delta_{ij})] \quad (7)$$

$$Q_{ji}^{TCSC} = -V_j^2 (B'_{ij} + B_{sh}) + V_i V_j [G'_{ij} \sin(\delta_{ij}) + B'_{ij} \cos(\delta_{ij})] \quad (8)$$

Where $G'_{ij} = \frac{r_{ij}}{r_{ij}^2 + (x_{ij} - x_c)^2}$;

$$B'_{ij} = \frac{-(x_{ij} - x_c)}{r_{ij}^2 + (x_{ij} - x_c)^2}$$

The change in the line flow due to series capacitance can be represented as a line without series capacitance with power injected at the receiving and sending ends of the line as shown in Figure.3. The real and reactive power injections at bus-*i* and bus-*j* can be expressed as:

$$P_{is}^{TCSC} = V_i^2 \Delta G'_{ij} - V_i V_j [\Delta G'_{ij} \cos \delta_{ij} + \Delta B'_{ij} \sin \delta_{ij}] \quad (9)$$

$$P_{js}^{TCSC} = V_j^2 \Delta G'_{ij} - V_i V_j [\Delta G'_{ij} \cos \delta_{ij} - \Delta B'_{ij} \sin \delta_{ij}] \quad (10)$$

$$Q_{is}^{TCSC} = -V_i^2 \Delta B'_{ij} - V_i V_j [\Delta G'_{ij} \sin \delta_{ij} - \Delta B'_{ij} \cos \delta_{ij}] \quad (11)$$

$$Q_{js}^{TCSC} = -V_j^2 \Delta B'_{ij} + V_i V_j [\Delta G'_{ij} \sin \delta_{ij} + \Delta B'_{ij} \cos \delta_{ij}] \quad (12)$$

Where $\Delta G'_{ij} = \frac{x_c r_{ij} (x_c - 2x_{ij})}{(r_{ij}^2 + x_{ij}^2)(r_{ij}^2 + (x_{ij} - x_c)^2)}$ and

$$\Delta B'_{ij} = \frac{-x_c (r_{ij}^2 - x_{ij}^2 + x_c x_{ij})}{(r_{ij}^2 + x_{ij}^2)(r_{ij}^2 + (x_{ij} - x_c)^2)}$$

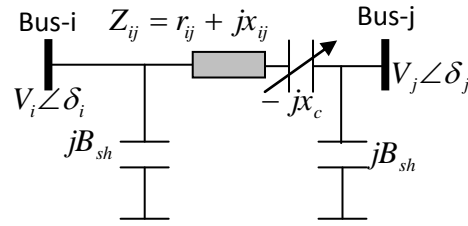


Figure 2. Model of TCSC.

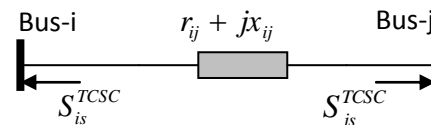


Figure 3. Injection Model of TCSC.

C. UPFC Model

The model of UPFC placed in lin-k connected between bus-*i* and bus-*j* is shown in figure.4. UPFC has three controllable parameters, namely, the magnitude and the angle of inserted voltage (V_T, ϕ_T) and the magnitude of the current (I_q). Based on the principle of UPFC and the vector diagram, the basic mathematical relations can be given as:

$$V_i' = V_i + V_T, \quad Arg(I_q) = Arg(V_i) \pm \frac{\pi}{2}$$

$$Arg(I_T) = Arg(V_i) \quad I_T = \frac{Re[V_T I_i^*]}{V_i} \quad (13)$$

The power flow equations from bus-*i* to bus-*j* and from bus-*j* to bus-*i* can be written as

$$S_{ij} = P_{ij} + jQ_{ij} = V_i I_{ij}^* = V_i (jV_i \frac{B}{2} + I_T + I_q + I_i)^* \quad (14)$$

$$S_{ji} = P_{ji} + jQ_{ji} = V_j I_{ji}^* = V_j (jV_j \frac{B}{2} - I_i)^* \quad (15)$$

The active and reactive power flow in the line having UPFC can be written, with (13)-(15), as

$$P_{ij}^{UPFC} = (V_i^2 + V_T^2) + 2V_i V_T g_{ij} \cos(\phi_T - \delta_i) - V_j V_T [g_{ij} \cos(\phi_T - \delta_j) + b_{ij} \sin(\phi_T - \delta_j)] \quad (16)$$

$$-V_i V_j (g_{ij} \cos \delta_{ij} + b_{ij} \sin \delta_{ij})$$

$$P_{ji}^{UPFC} = V_j^2 g_{ij} - V_j V_T [g_{ij} \cos(\phi_T - \delta_j) - b_{ij} \sin(\phi_T - \delta_j)] - V_i V_j (g_{ij} \cos \delta_{ij} - b_{ij} \sin \delta_{ij}) \quad (17)$$

From basic circuit theory, the injected equivalent circuit of figure.5 can be obtained. The injected active and reactive power at bus-i and bus-j and reactive powers of a line having a UPFC are:

$$Q_{ij}^{UPFC} = -V_i I_q - V_i^2 [b_{ij} + \frac{B}{2}] + V_i V_T [(g_{ij} \sin(\phi_T - \delta_j)] + (b_{ij} + \frac{B}{2}) \cos(\phi_T - \delta_i)] - V_i V_j (g_{ij} \sin \delta_{ij} - b_{ij} \cos \delta_{ij}) \quad (18)$$

$$Q_{ji}^{UPFC} = -V_j^2 (b_{ij} + \frac{B}{2}) + V_j V_T [g_{ij} \sin(\phi_T - \delta_j) + b_{ij} \cos(\phi_T - \delta_j)] + V_j V_i (g_{ij} \sin \delta_{ij} + b_{ij} \cos \delta_{ij}) \quad (19)$$

From basic circuit theory, the injected equivalent circuit of figure.5 can be obtained. The injected active and reactive power at bus-i and bus-j and reactive powers of a line having a UPFC are:

$$P_{is}^{UPFC} = -V_T^2 g_{ij} - 2V_i V_T g_{ij} \cos(\phi_T - \delta_i) + V_j V_T [g_{ij} \cos(\phi_T - \delta_j) + b_{ij} \sin(\phi_T - \delta_j)] \quad (20)$$

$$P_{js}^{UPFC} = V_j V_T [g_{ij} \cos(\phi_T - \delta_j) - b_{ij} \sin(\phi_T - \delta_j)] \quad (21)$$

$$Q_{is}^{UPFC} = V_i I_q + V_i V_T [g_{ij} \sin(\phi_T - \delta_i) + (b_{ij} + \frac{B}{2}) \cos(\phi_T - \delta_i)] \quad (22)$$

$$Q_{js}^{UPFC} = -V_j V_T [g_{ij} \sin(\phi_T - \delta_j) + b_{ij} \cos(\phi_T - \delta_j)] \quad (23)$$

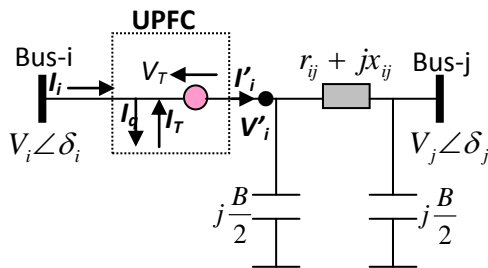


Figure 4. Model of UPFC

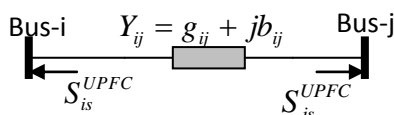


Figure 5. Injection model of UPFC.

III. MULTI-OBJECTIVE OPTIMIZATION

In a MOP, there may not exist one solution that is best with respect to all objectives. Usually, the aim is to determine the trade-off surface, which is a set of nondominated solution points, known as Pareto optimal solutions. Every individual in this set is an acceptable solution.

For any two X_1 and X_2 , we can have one of two possibilities : one dominates the other or none dominates the other. In a minimization problem, we say that the solution X_1 dominates X_2 , if the following two conditions are satisfied [7] :

$$\left\{ \begin{array}{l} \forall i \in \{1, 2, \dots, N_{obj}\}, f_i(X_1) \leq f_i(X_2) \\ \exists j \in \{1, 2, \dots, N_{obj}\}, f_j(X_1) < f_j(X_2) \end{array} \right. \quad (24)$$

Where :

N_{obj} : Number of objective functions.

f_i : ith objective function.

The goal of a multi-objective optimization algorithm is not only to guide the search towards the Pareto optimal front, but, also to maintain population diversity in the set of the nondominated solutions.

In the rest of this section, we will present the elitist MOEA NSGAII. So, we must be start with a presentation of the NSGA approach.

A. NSGA approach

The basic idea behind NSGA is the ranking process executed before the selection operation. The ranking procedure consists to find the nondominated solutions in the current population P . These solutions represent the first front F_1 . Afterwards, this first front is eliminated from the population and the rest is processed in the same way to identify nondominated solutions for the second front F_2 . This process continues until the population is properly ranked. So, can write [8] :

$$P = \bigcup_{j=1}^r F_j$$

Where, r is the number of fronts.

The same fitness value f_k is assigned to all of individuals of the same front F_k . This fitness value decreases while passing from the front F_k to the F_{k+1} . To maintain diversity in the population, a sharing method is used. Let consider d_{ij} the variable distance (Euclidean norm) between two solutions \underline{X}_i and \underline{X}_j .

$$d_{ij} = \sqrt{\sum_{k=1}^S \left(\frac{X_k^{(i)} - X_k^{(j)}}{X_k^{max} - X_k^{min}} \right)^2} \quad (25)$$

Where S is the number of variables in the MOP. The parameters X_k^{max} and X_k^{min} respectively the upper and lower bounds of variable X_k .

$$\underline{X}_i = (X_1^{(i)}, X_2^{(i)}, \dots, X_S^{(i)}) \quad (26)$$

The sharing procedure is as follows :

Step 1 : Fix the niche radius σ_{share} and a small positive number ε .

Step 2 : Initiate $f_{min} = N_{pop} + \varepsilon$ and the counter of front $j = 1$.

Step 3 : From the r nondominated fronts F_j which constitute P .

$$P = \bigcup_{j=1}^r F_j$$

Step 4 : For each individual $\underline{X}_q \in F_j$:

- associate the dummy fitness $f_j^{(q)} = f_{min} - \varepsilon$;

- calculate the niche count n_{cq} as given in [8] ;
- calculate the shared fitness $f_j^{(q)} = \frac{f_j^{(q)}}{n_{cq}}$.

Step 5 : $F_{\min} = \min(F_j^{(q)}; q \in P_j)$ and $j = j + 1$.

Step 6 : If $j \leq r$, then, return to step 4. Else, the process is finished.

The MOEAs using nondominated sorting and sharing have been criticized mainly for their $O(MN^3)$ computational complexity (M is the number of objectives and N is the population size). Also, these algorithms are not elitist approaches and they need to specify the sharing parameter. To avoid these difficulties, we present in the following an elitist MOEA which is called Nondominated Sorting Genetic Algorithm II (NSGAI).

B. NSGAI approach

In this approach, the sharing function approach is replaced with a crowded comparison. Initially, an offspring population Q_t is created from the parent population P_t at the t th generation. After, a combined population R_t is formed [8].

$$R_t = P_t \cup Q_t$$

R_t is sorted into different no domination levels F_j as shown in the NSGA approach. So, we can write :

$$R_t = \bigcup_{j=1}^r F_j, \text{ where, } r \text{ is number fronts.}$$

Finally, one iteration of the NSGAI procedure is as follows :

Step 1 : Create the offspring population Q_t from the current population P_t .

Step 2 : Combine the two population Q_t and P_t to form R_t .

Step 3 : Find the all nondominated fronts F_i and R_t .

Step 4 : Initiate the new population $P_{t+1} = \emptyset$ and the counter of front for inclusion $i = 1$.

Step 5 : While $|P_{t+1}| + |F_i| \leq N_{pop}$, do :

$$P_{t+1} \leftarrow P_{t+1} \cup F_i$$

$$i \leftarrow i + 1$$

Step 6 : Sort the last front F_i using the crowding distance in descending order and choose the first $(N_{pop} - |P_{t+1}|)$ elements of F_i .

Step 7 : Use selection, crossover and mutation operators to create the new offspring population Q_{t+1} of size N_{obj} .

To estimate the density of solution surrounding a particular solution X_i in a nondominated set F , we calculate the crowding distance as follows:

Step 1 : Let's suppose $q = |F|$. For each solution X_i in F , set $d_i = 0$.

Initiate $m = 1$.

Step 2 : Sort F in the descending order according to the objective function of rank m .

Let's consider $I^m = \text{sort}_{[f_m >]}(F)$ the vector of indices, i.e. I_i^m is the index of the solution X_i in the sorted list according to the objective function of rank m .

Step 3 : For each solution X_i which verifies $2 \leq I_i^m \leq (q - 1)$, update the value of d_i as follows:

$$d_i \leftarrow d_i + \frac{f_m^{I_i^{m+1}} - f_m^{I_i^{m-1}}}{f_m^{\max} - f_m^{\min}} \quad (27)$$

Then, the boundary solutions in the sorted list (solutions with smallest and largest function) are assigned an infinite distance value, i.e. if, $I_i^m = 1$ or $I_i^m = q$, $d_i = \infty$.

Step 4 : If $m = M$, the procedure is finished. Else, $m = (m + 1)$, and return to step 2.

C. Implementation of the NSGAI

The proposed NSGAI has been implemented using real-coded genetic algorithm (RCGA)[7]. So, a chromosome X corresponding to a decision variable is represented as a string of real values x_i , i.e.

$X = x_1 x_2 \dots x_{lchrom}$. $lchrom$ is the chromosome size and x_i is a real number within its lower limit a_i and

upper limit b_i . i.e. $x_i \in [a_i, b_i]$. Thus, for two individuals having as chromosomes respectively X and Y and after generating a random number

$\alpha \in [0, 1]$, the crossover operator can provide two chromosomes X' and Y' with a probability P_C as follows [8] :

$$X' = \alpha X + (1 - \alpha)Y$$

$$Y' = (1 - \alpha)X + \alpha Y \quad (28)$$

In this study, the non-uniform mutation operator has been employed. So, at the t th generation, a parameter x_i of the chromosome X will be transformed to other parameter x'_i with a probability P_m as follows :

$$x_i' = \begin{cases} x_i + \Delta(t, b_i - x_i), & \text{if } \tau = 0 \\ x_i - \Delta(t, x_i - a_i), & \text{if } \tau = 1 \end{cases} \quad (29)$$

$$\Delta(t, y) = y \left(1 - r^{(1-t/g_{max})^\beta} \right) \quad (30)$$

Where τ is random binary number, r is a random number $r \in [0,1]$ and g_{max} is the maximum number of generations. β is a positive constant chosen arbitrarily.

IV. PROBLEM FORMULATION

A. Problem formulation

The optimal VAR dispatch problem is to optimise the steady performance of a power system in terms of one or more objective functions while satisfying several equality and inequality constraints. In this section, we suppose that the extremities FACTS devices are referred by bus i and j .

B. Objective functions

• Real power loss

This objective consists to minimise the real power loss P_L in transmission lines that can be expressed as [1] :

$$P_L = \sum_{k=1}^{N_b} P_k$$

Where :

$$P_k = \begin{cases} P_{i,SSSC} \text{ or } P_{i,UPFC} & \text{if } k = i \\ P_{j,SSSC} \text{ or } P_{j,UPFC} & \text{if } k = j \\ \sum_{h=1}^{N_b} V_k V_h Y_{kh} \cos(\alpha_k - \alpha_h - \theta_{kh}), & \text{if } k \neq i, j \end{cases} \quad (31)$$

N_b : number of buses;

$V_k \angle \alpha_k$ and $V_h \angle \alpha_h$: respectively voltages at bus k and h ;

Y_{kh} and θ_{kh} : respectively modulus and argument of the kh -th element of the nodal admittance matrix Y .

• Voltage deviation

This objective is to minimize the deviation in voltage magnitude at load buses that can be expressed as :

$$V_D = \sum_{i=1}^{N_L} |V_i - V_i^{ref}| \quad (32)$$

Where :

N_L : number of load buses;

V_i^{ref} : prespecified reference value of the voltage magnitude at the i -th load bus.

V_i^{ref} is usually set to be 1.0 pu.

C. Problem constraints

• Equality constraints

These constraints represent typical load flow equations as follows :

$$P_{Gi} - P_{Di} - \sum_{j=1}^N V_j \left[G_{ij} \cos(\alpha_i - \alpha_j) + B_{ij} \sin(\alpha_i - \alpha_j) \right] = 0 \quad (33)$$

$$Q_{Gi} - Q_{Di} - \sum_{j=1}^N V_j \left[G_{ij} \sin(\alpha_i - \alpha_j) - B_{ij} \cos(\alpha_i - \alpha_j) \right] = 0 \quad (34)$$

Where :

P_{Gi} and Q_{Gi} : generator real and reactive power at i -th bus, respectively;

P_{Di} and Q_{Di} : load real and reactive power at i -th bus, respectively;

G_{ij} and B_{ij} : transfer conductance and susceptance between buses i and j , respectively.

• Inequality constraints

These constraints represent are :

a) Voltage stability limits

The voltage collapse point or critical point (VCP) shown in Figure 6, is defined by the maximum power transfer to a load at bus i without violating voltage stability limits. VCP at the load bus i must be less than or equal to one.

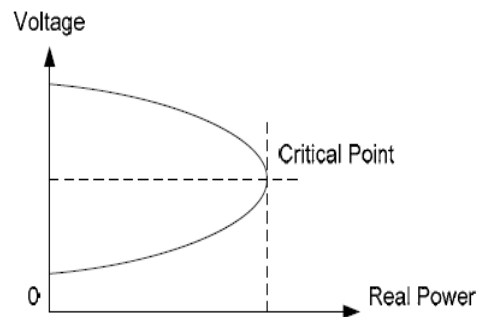


Figure 6. Power-Voltage Curve

$$VCP \leq 1 \quad (35)$$

b) Security constraints

These include the constraints of voltage at load buses V_L as follows:

$$V_{Li}^{\min} \leq V_{Li} \leq V_{Li}^{\max}, i = 1, \dots, N_L \quad (36)$$

c) FACTS devices constraints :

The FACTS devices limit is given by:

$$-0.5X_L < x_c < 0.5X_L \quad (37)$$

$$-200MVAR \leq Q_{UPFC} \leq 200MVAR \quad (38)$$

Where :

X_L : Original line reactance in (pu).

x_c : Reactance added to the line where TCSC is placed in (pu)

Q_{UPFC} : reactance power injected at UPFC placed in MVAR.

V. IEEE 30-BUS TEST SYSTEM

Figure 7 shows the IEEE 30-bus system which consists of 6 generator buses, 24 load buses and 41 transmission lines of which 4 branches (6–9), (6–10), (4–12), and (28–27) are with the tap setting transformer. The transmission line parameters of this system and the base loads are taken from [9]. For the RPD problem, the candidate buses for reactive power compensation are 10, 12, 15, 17, 20, 21, 23, 24, and 29. The lower voltage magnitude limits at all buses are 0.95 p.u. and the upper limits are 1.1 for all the PV buses and 1.05 p.u. for all the PQ buses. The lower and upper limits of the transformer in tappings are 0.9 and 1.1 p.u. respectively. Considering a base power of 100 MVA for the overall system and base voltages of 100 KV.

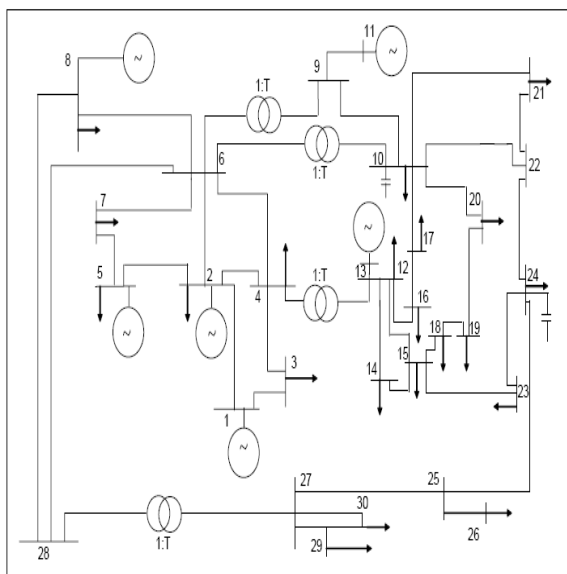


Figure: 7 IEEE 30 bus systems

In this work, four branches, (6, 10),(4, 12), (10, 22) and (28, 27) are installed with UPFC and three branches, (1, 3), (3, 4) and (2, 5) are installed with TCSC. The best location of FACTS devices for the optimal case is the branche (10,22) for UPFC and the branche (2,5) for the TCSC.

Figure 8 and 9 shows the convergence of the voltage deviation and power loss respectively to 0.172 pu and 4.447MW with UPFC, and 0.183 pu and 4.512 MW with TCSC.

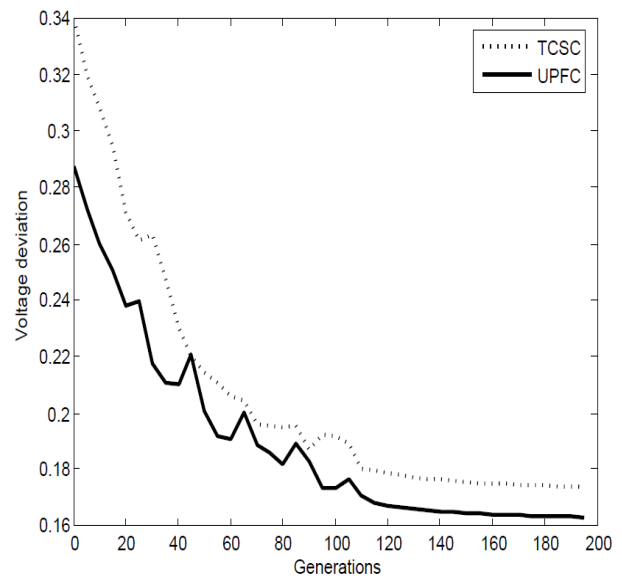


Figure 8 : Convergence of voltage deviation objective with FACTS devices.

In the figure.9, the red curve indicates the effect of the UPFC, the blue curve illustrates the effect of the TCSC. we can say that the UPFC has the most significant effect compared to TCSC.

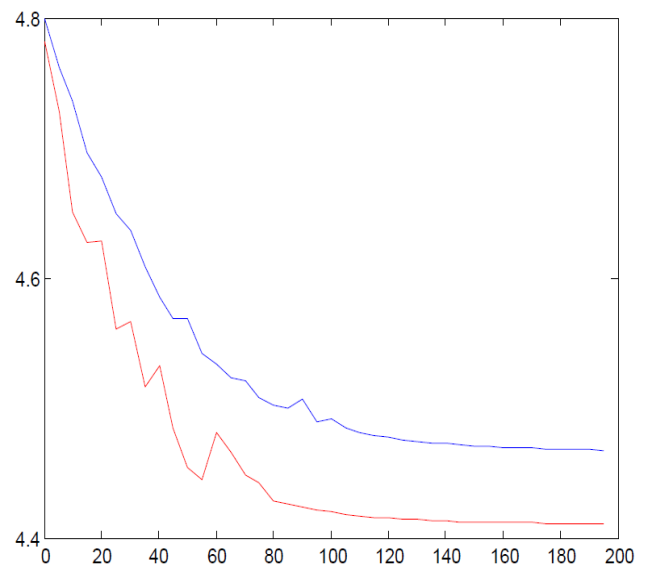


Figure 9 : Convergence of power loss objective with FACTS devices

The diversity of the pareto optimal set over the trade off surface is shown in figure 10.

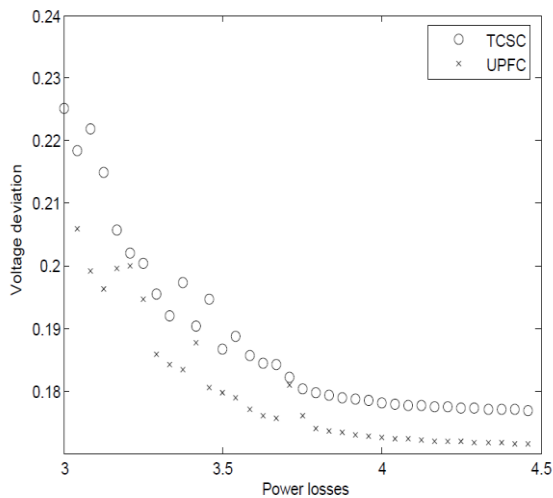


Figure 10: Pareto-optimal front of the proposed approach

Figure 11 provides voltage magnitude of all buses obtained from TCSC and UPFC.

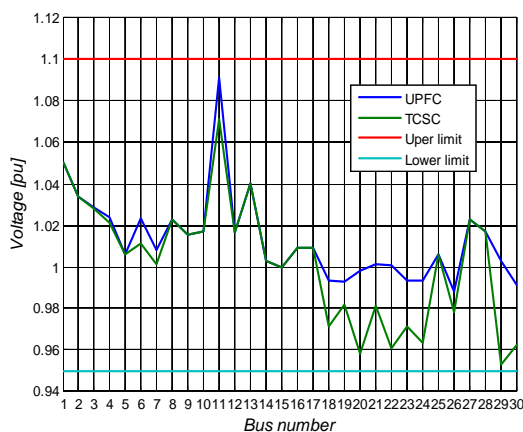


Figure 11 : Voltage profile with TCSC and UPFC

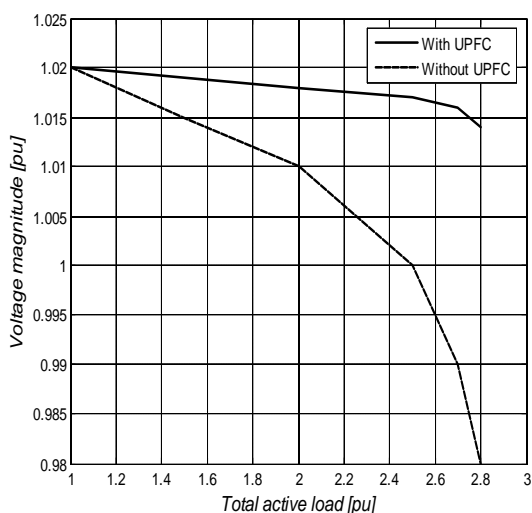


Figure 12. P-V curves at load bus 29

According to Figure 11, we see very well that the bus 29 is the load bus that has the largest voltage variation, because it is very far from the generator buses. Figure 12 shows the effect of UPFC in improving the stability of the latter power.

VI. CONCLUSION

This paper presents the application of NSGAI technique to find the optimal location of FACTS devices for minimizing simultaneously real power loss in transmission lines and voltage deviation in order to obtain the better voltage stability at load buses, under several equality and inequality constraints. An existing Newton-Raphson algorithm is modified to include FACTS devices is used to solve load flow equations.

The FACTS devices can provide control of voltage magnitude, voltage phase angle and impedance. Therefore, it can be utilized to effectively increase power transfer capability of the existing power transmission lines, since it reduces considerably the real power losses. The NSGAI achieves better solution for the voltage stability with UPFC than TCSC fixed at the given locations.

The simulation results obtained for the IEEE-30 bus network showed the effectiveness of the proposed method. This approach is able to give several possible solutions simultaneously. These solutions are presented by Pareto-optimal front. Also, this method does not impose any limitation on the number of objectives, constraints.

REFERENCES

- [1] M. A. Abido, J. M. Bakhshwain, 'Optimal VAR dispatching using a multiobjective evolutionary algorithm', *Electrical Power and Energy System*, 27 (2005) pp. 13-20.J.
- [2] Mansour MO, Abdel-Rahman TM, Non-linear VAR optimization using decomposition and coordination. *IEEE Trans Power Apparatus Syst* 1984; PAS-103(2):246-55.
- [3] Mamandur KRC, Chnoweth RD. Optimal control of reactive power flow for improvement in voltage profiles and for real power loss minimization. *IEEE Trans Power Apparatus Syst*. 1981; PAS-100(7):3185-93.
- [4] Iba K. Reactive power optimization by genetic algorithm. *IEEE Trans Power Syst*. 1994;9(2):685-92.
- [5] Abido MA. A novel multiobjective evolutionary algorithm for environmental/economic power dispatch. *Electr Power Syst Res* 2003;65(1):71-81..
- [6] Verma K.S., Singh S.N., Gupta H.O., 2001.FACTS devices location for enhancement of total transfer capability,

- Power Engineering Society Winter Meeting, IEEE, Vol.2:522-527.*
- [7] A.H.F.Dias and J.A..Vasconcelos, Multi-objective genetic algorithms applied to solve optimization problems, *IEEE Trans. On Magnetics, Vol. 38, No. 2, pp. 1133-1136,2002..*
- [8] F.Herrera, M.Lozano and J.L. Verdegay, Tackling real-coded genetic algorithm:operators and tools for behavioural analysis, *Artif. Intell. Rev, Vol. 12, No. 4, pp.265-319,1998.*
- [9] *The arabic Journal for science and engineering, volume 34, Number 2B.* S.Durairaj and D.Devaraj. April 2009.